〈일반논문〉
Journal of the Korean Society of Visualization, Vol. 20, No. 3 (102~108), 2022
(Manuscript received : 2022.10.21./Revised : 2022.11.16./Accepted : 2022.11.16.)
DOI:http://dx.doi.org/10.5407/jksv.2022.20.3.102

ISSN 1598-8430 Print
ISSN 2093-808X Online

냉장고 팬 모듈의 물빠짐 구멍 주변 유동 특성 검증

판진싱* · 이수환** · 서희림* · 김동우* · 염은섭†

Flow characteristics validation around drain hole of fan module in refrigerator

Jinxing Fan*, Suhwan Lee**, Heerim Seo*, Dongwoo Kim* and Eunseop Yeom†

Abstract In the fan module of the intercooling refrigerator, a drain hole structure was designed for stable drainage of defrost water. However, the airflow passing through the drain hole can disturb flow features around the evaporator. Since this backflow leads to an increase in flow loss, the accurate experimental and numerical analyses are important to understand the flow characteristics around the fan module. Considering the complex geometry around the fan module, three different turbulence models (Standard k-ε model, SST k-ω model, Reynolds stress model) were used in computational fluid dynamics (CFD) analysis. According to the quantitative and qualitative comparison results, the Standard k-ε model was most suitable for the research object. High-accuracy results well match with the experiment result and overcome the limitation of the experiment setup. The method used in this study can be applied to a similar research object with an orifice outflow driven by a rotating blade.

Key Words : Flow Visualization(유동가시화), Particle Image Velocimetry(입자영상유속계), CFD Simulation(전산유체역학), Turbulence Model(난류 모델)

1. Introduction

The intercooling refrigerator with a forced air convection cooling system was favored in the market because of its multi-temperature zones and frost-free function.(1) The cooling capacity of a refrigerator was determined by the heat transfer between the evaporator and airflow driven by a refrigerator fan (R-fan) module. A special structure of "Drain hole" was designed at the bottom of the fan module for discharging the defrost water from the fan module to the evaporator. High humidity air induced by the humidity change during the opening and closing of the door forms frost layers over the evaporator and inside the R-fan module.(2) The airflow passing through the drain hole of the R-fan module can form a vortex shape backflow with the effect of the fan blade rotation and then affect the airflow around the evaporator. The cooling capacity of the refrigerator was mainly related to the airflow states, so it was important to investigate the flow characteristics around the R-fan module.(3-5)

† School of Mechanical Engineering, Pusan National University (PNU), Associate Professor
E-mail: esyeom@pusan.ac.kr
* School of Mechanical Engineering, PNU, MS student.
** School of Mechanical Engineering, PNU, PhD student

The research area around the fan module consisted of a rotation body, lamellar fin, and slit structure. The comparison of numerical results with the flow visualization method was a good approach in order to finding the best numerical models for each study.[6-7] In this study, three turbulence models were adopted to investigate the flow characteristics with a complex geometry structure, including the standard k-ε model, the shear stress transport (SST) k-ω model, and the Reynolds stress model. The standard k-ε model, proposed by Launder and Spalding,[8] independently determined the turbulent velocity and length scales. This model had become the workhorse of practical engineering flow calculations with the advantage of Robustness, economy, and reasonable accuracy in industrial flow and heat transfer simulations.[9-10] The SST k-ω model combined the merits of the k-ε model and the k-ω model, and the stable algorithm and high accuracy can be obtained near the wall.[11-12] The Reynolds stress model was the most elaborate type of turbulence model of Fluent, which can account for the effects of streamline curvature, swirl, rotation, and rapid changes in strain rate in a more rigorous manner and had greater potential to give accurate predictions for complex flows.[13-14]

For experimental validation of three turbulence models, particle image velocimetry (PIV) technique was adopted. The backflow induced by the drain hole and velocity distribution were quantitatively and qualitatively analyzed to ensure the accuracy of the research.

2. Materials and methods

2.1 Physical model

Fig. 1 showed a 1:1 size refrigerator product 3D model containing the refrigerator fan module and evaporator module. The drain hole structure can be found under the fan module designed for stable

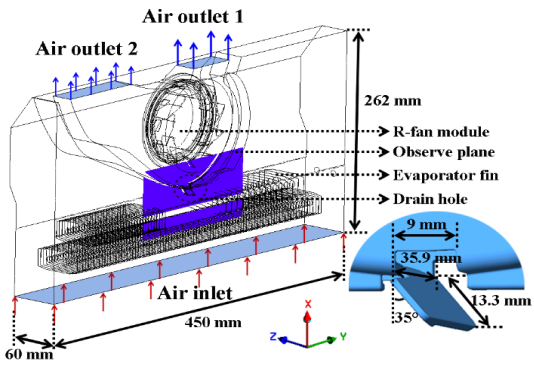

Fig. 1. Simulation domain around R-fan module.

drainage of defrost water. The depth and width of the rectangular hole were 9 mm and 35.9 mm. The flow guide for the backflow direction had a length of 13.3 mm and an angle of 35° from the vertical line. PIV experiments were conducted in a visualization chamber (340 mm × 460 mm × 68 mm) consisting of acrylic sheets. To mimic the conditions around the evaporator, transparent acrylic tubes and sheets were installed below the R-fan module. Rotation speed of R-fan was accurately controlled by the personal computer to be 1,200 RPM (round per minute).

In CFD domain, plane with a dimension of 180 mm×90 mm was extracted to investigate the flow jet from the drain hole. The air circulation inside the research domain was driven by an R-fan module with 1,200 RPM.

2.2 Experimental method

To investigate the flow features around the drain hole of the fan module, the PIV method was adopted to visualize the velocity distribution. The PIV experiment system consisted of a laser with 5 W power and wavelength of 532 nm (MGL-F-532, CNI Co., Ltd., China), a high-speed camera (Phantom VEO710L, Vision Research Inc., USA), and a data-processing computer. The experiment setup was same as the real working conditions

with a 1,200 RPM fan and using air as working fluid with properties shown in **Table 1.** The olive oil particles with a mean diameter of 1 μm, generated using a Laskin nozzle, were seeded with the airflow. The flowing image in the research area was captured with a size of 1,280×800 pixels and 5,000 fps (frame per second).

Table 1. Properties of working fluid.

	Viscosity (kg/m·s)	Density (kg/m^3)
Air	1.7894×10^{-5}	1.225

The velocity vector fields were extracted using PIV technique with a cross-correlation algorithm based on the fast Fourier transform. An interrogation window size of 32 pixels by 32 pixels with 50% overlap was applied. Time-averaged vector field was obtained by averaging 5,000 PIV results. For filtering error values, a Gaussian filter was applied.

2.3 Numerical method

The commercial software ANSYS Fluent 2020 R2 was selected as the tool for the CFD simulation. The SIMPLEC algorithm was selected to couple the pressure and velocity. All equations were solved by the second-order upwind discretization scheme. The criterion for convergence was that the monitored parameters (mass flow rate, velocity) of the inlet and outlet should be steady. There were many turbulence models that can be used in CFD simulation in the preliminary tests, but the emphasis and accuracy should be considered in advance. To validate CFD turbulence models, Standard k-ε, SST k-ω, and Reynolds stress models were compared. The boundary conditions were set as atmospheric pressure inlet and pressure outlet with an R-fan rotating at 1,200 RPM inside CFD domain. The working fluid was air same as in the PIV experiment.

The mesh in the CFD domain was generated by ANSYS Mesh software. A mesh independence test was conducted to find the proper grid numbers (the relative deviations of the flow rate at air outlet positions were within 0.5%). The grid numbers of about 15.6 million were selected. The evaporator tubes ($D_o = 8$ mm) with aluminum refrigerant rectangular shape fins (60 mm × 27 mm × 0.18 mm) were also modeled. The distance between the fins was 5 mm.

3. Results and discussion

In this study, the flow characteristics around the drain hole of the R-fan module obtained by CFD simulation with the turbulence models were compared with that obtained by the PIV experiment.

3.1 Velocity distribution of PIV and CFD results

The local velocity distribution was fundamental to validating the flow characteristics of different turbulence models. **Fig. 2** showed the local velocity distributions at the observe plane described in **Fig. 1**. For a clear comparison, a black mask same as the PIV post-processing was applied to the simulation results. From the PIV experiment result, an air backflow can be found flowing through the drain hole of the R-fan module. Specifically, some airflows induced by the rotation of the R-fan flowed out through the drain hole following a guide structure. Below the drain hole, fins were not installed at a distance of 10 mm to prevent severe frost accumulation.

In experimental results, the velocity magnitude near the drain hole was somewhat low. It may be mainly affected by the black mask and insufficient laser illumination blocked by the guide. The backflow passing through the drain hole expanded and then extended to the evaporator fin and tube. Due to the solid surface, jet-like backflow can be bounced. In addition, updraft flow derived by the

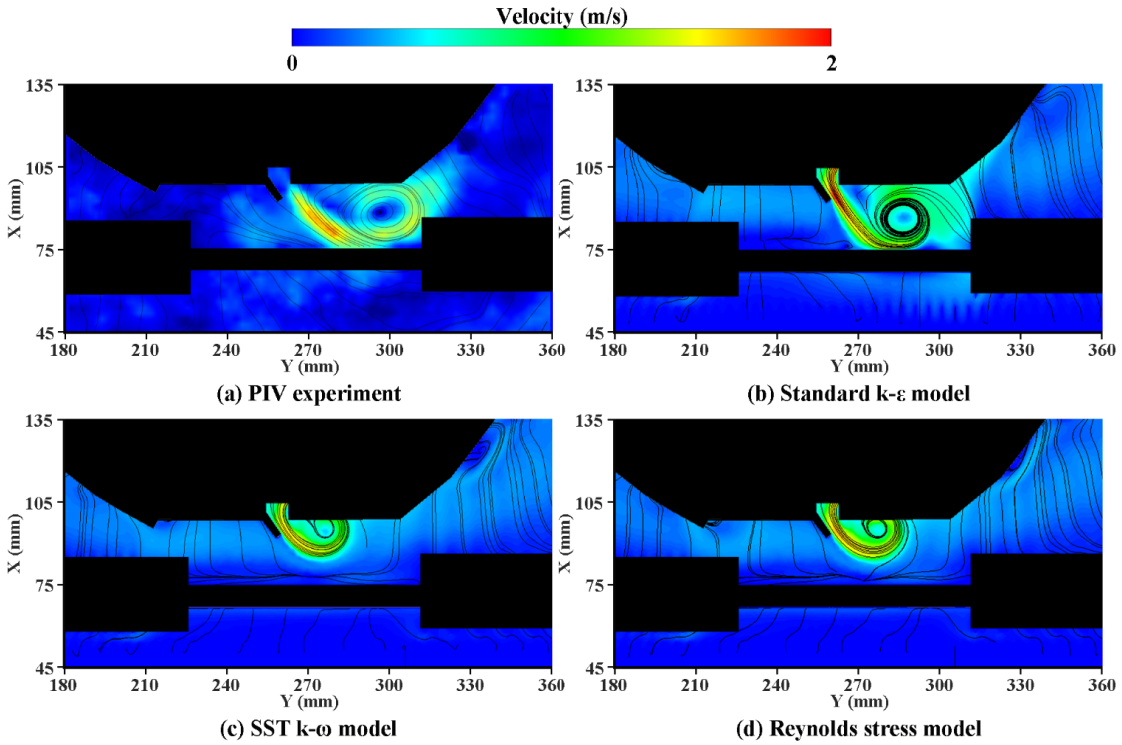

Fig. 2. Comparison of (a) experimental vector field and (b-c) CFD simulation results.

rotation of the R-fan accentuated the circulatory flow. Similarly, the circulatory flow can be seen as an orifice outflow with a rotating condition.

In all CFD simulation results, the circulatory flow can be observed. However, the velocity distributions including strength and size of the circulatory flow were somewhat different between experimental results and CFD results. From the result of the Standard k-ε model, the shape of the circulatory flow was more similar to the PIV experiment result. However, the backflow can be propagated along the evaporator tube in the PIV experiment result. In the cases of the other two models, even though a similar backflow appeared, the backflow center position was higher than the PIV experiment result. In addition, there was no clear tendency extended to the evaporator tube for the results with the SST k-ω and Reynolds stress models.

As for the velocity value, the maximum velocity appeared in the Standard k-ε model with a value of 1.99 m/s, at the drain hole central position. At the same position, the velocity of the SST k-ω model was 1.59 m/s and 1.69 m/s of the Reynolds stress model. While at the PIV experiment result, the maximum velocity was 1.75 m/s due to the aforementioned problems. From the velocity distribution comparison, the Standard k-ε model was the most suitable turbulence model to describe the flow features below the drain hole.

3.2 Characteristics of circulatory flow

For quantitative comparison of the PIV experiment and CFD simulation result, the velocity profile with absolute value at the central line of the circulatory flow was extracted along the X-axis as shown in **Fig. 3**. The circulatory flow central line Y-axis

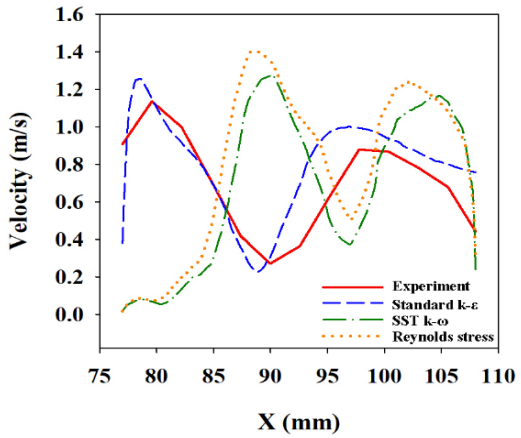

Fig. 3. Velocity profiles along the central line of circulatory flow.

locations were Y = 297 mm, Y = 287 mm, Y = 276 mm, and Y = 277 mm for the experiment, Standard k-ε, SST k-ω and Reynolds stress models, respectively. As X increased, the position was moved to the drain hole from the evaporator tube. Due to jet-like backflow, the maximum velocity position in the profile was observed at the low X-axis. As approaching the center position of circulatory flow, velocity decreased. After the center position, velocity increased up to the second peak with a relatively low value compared to each maximum value. Since the positions of the circulatory flow center were different among cases, the valley points were positioned in the range of X = 88-98 mm. The velocity plot of the PIV experiment and the Standard k-ε model corresponded well in terms of variation tendency and the center position. The error of the valley position velocity was 15.9%, and the average error at peak positions was 12.2%. As for the SST k-ω model and Reynolds stress model, the velocity valley position was far away from the evaporator tube caused by the weak jet flow. It showed a significant discrepancy from the experimental result.

Overall, the characteristics and velocity value of circulatory flow indicated the Standard k-ε model was more suitable compared to the other models. The discrepancy of the valley position and peak value may be caused by the influence of turbulence anisotropy, the difference in resolution of the interaction window size setting to extract the velocity, and the filter setting for removing the error vectors.[15]

3.3 3D streamlines distribution

After validation of CFD turbulence models, 3D streamlines from the air inlet and inside the R-fan module were shown in **Fig. 4**. The streamlines from the air inlet flowed to the center of the R-fan module due to the rotation of the fan blade (**Fig. 4a**). From the streamlines shown in **Fig. 4b**, the streamlines mainly flowed outside through two air outlet positions, while a clear vortex backflow can be found flowing through the drain hole with a relatively high velocity corresponding with the experiment result in **Fig. 2a**. The discharged air from the fan domain mixed with the updraft and flowed into the fan domain again. It was noteworthy that the updraft around the drain hole showed an irregular flow state caused by the disturbance of backflow, which may affect the performance of the refrigerator.

4. Conclusions

In this paper, the PIV experiment and CFD simulation method were used to investigate the flow characteristics around the R-fan module. The circulatory flow passing through the drain hole was a representative flow characteristic of the fan module with a similar structure, which can be seen as an orifice outflow with a rotating condition. Three turbulence models were used to validate the PIV experiment result. The backflow and velocity plots were extracted to discuss which turbulence models were more suitable for this study. The

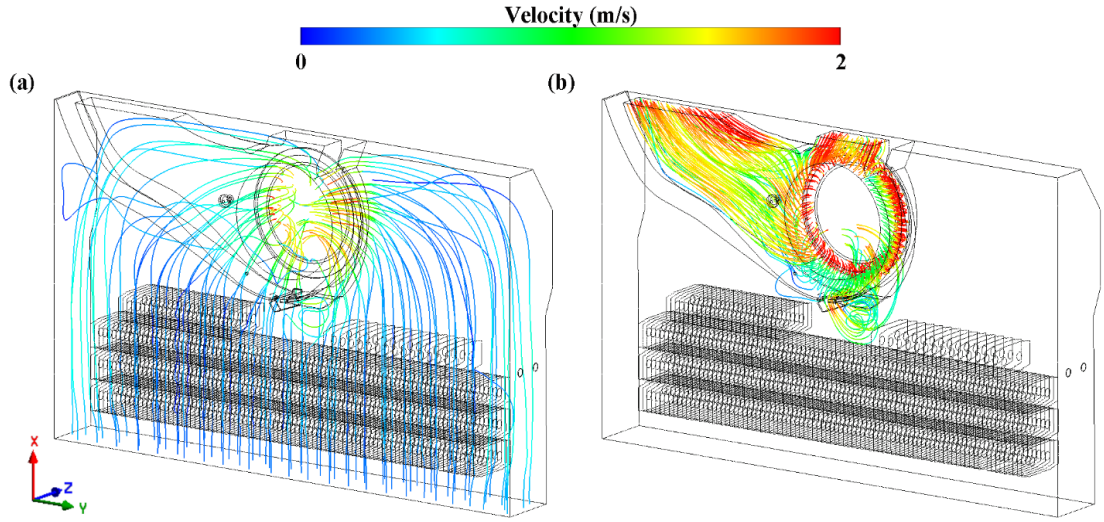

Fig. 4. Streamlines distribution (a) from air inlet and (b) inside R-fan module.

following conclusions can be drawn from the comparison of the results.

(1) The air discharged from the R-fan module formed backflow with the effect of a guide structure.

(2) The standard k-ε turbulence model well matched with the PIV experiment result with a similar airflow characteristic and velocity variation trend. The results showed the circulatory flow was fully developed and expanded to the evaporator side. The SST k-ω and Reynolds stress models were not suitable for the rotating flow simulation.

(3) According to the result comparison, there were some errors induced by the limitation of the experiment setup and post-processing. The simulation method can be used to reduce the error with a reliable result.

Acknowledgments

This work was supported by a 2-Year Research Grant of Pusan National University.

REFERENCE

1) James, C., Onarinde, B. A. and James, S. J., 2017, “The use and performance of household refrigerators: A review,” Comprehensive Reviews in Food Science and Food Safety, Vol. 16(1), pp. 160-179.

2) Kang, S., Kim, D., Lee, S., Kang, D. and Yeom, E., 2021, “Design of drain tube with movable shutter in household refrigerators,” International Journal of Refrigeration, Vol. 130, pp. 76-86.

3) Cui, P., He, L. and Mo, X., 2022, “Flow and heat transfer analysis of a domestic refrigerator with complex wall conditions,” Applied Thermal Engineering, Vol. 209, pp. 118306.

4) Ye, J., Huang, X. and Cheng, Y., 2020, “Air volume improvement in the duct system in frost-free refrigerators based on the CFD method,” J Supercomput, Vol. 76, pp. 3749-3764.

5) Meng, X. and Yu, B., 2009, “Experimental research on air flow performance at supply-air openings in frost-free refrigerator by DPIV,” Applied thermal engineering, Vol. 29(16), pp. 3334-3339.

6) Zhou, L., Bai, L., Li, W., Shi, W. and Wang,

C., 2018, “PIV validation of different turbulence models used for numerical simulation of a centrifugal pump diffuser,” Engineering computations, Vol. 35, pp. 2-17.
7) Hong, H., An, S. H., Seo, H., Song, J. M. and Yeom, E., 2021, “Flow Characteristics in a Human Airway model for Oral Cancer Surgery by PIV Experiment and Numerical Simulation,” Journal of the Korean Society of Visualization, Vol. 19(3), pp.115-122.
8) Launder, B. E. and Spalding, D. B., 1972, “Lectures in mathematical models of turbulence.”
9) Feng, J., Benra, F. K. and Dohmen, H. J., 2010, “Application of different turbulence models in unsteady flow simulations of a radial diffuser pump,” Forschung im Ingenieurwesen, Vol. 74(3), pp. 123-133.
10) Gagan, J., Smierciew, K., Butrymowicz, D. and Karwacki, J., 2014, “Comparative study of turbulence models in application to gas ejectors,” International Journal of Thermal Sciences, Vol. 78, pp. 9-15.
11) Zhang, L. and Che, D., 2011, “Turbulence models for fluid flow and heat transfer between cross-corrugated plates,” Numerical Heat Transfer, Part A: Applications, Vol. 60(5), pp. 410-440.
12) Dhakal, T. P. and Walters, D. K., 2011, “A three-equation variant of the SST k-ω model sensitized to rotation and curvature effects,” Journal of Fluids Engineering, Vol. 133(11), pp. 111201.
13) Bernard, P. S., Thomas, J. M. and Handler, R. A. 1993, “Vortex dynamics and the production of Reynolds stress,” Journal of Fluid Mechanics, Vol. 253, pp. 385-419.
14) Jawarneh, A. M. and Vatistas, G. H., 2006, “Reynolds stress model in the prediction of confined turbulent swirling flows.” Vol. 128(6), pp. 1377-1382.
15) Xu, X., Wu, J., Weng, W. and Fu, M., 2020, “Investigation of inhalation and exhalation flow pattern in a realistic human upper airway model by PIV experiments and CFD simulations,” Biomechanics and modeling in mechanobiology, Vol. 19(5), pp. 1679-1695.